Nanotechnology **17** (2006) 2073–2077 doi:10.1088/0957-4484/17/8/046

Visible light emission from innate silicon nanocrystals in an oxide matrix grown at low temperature

Z X Cao, R Song, L B Ma, Y Du, A L Ji and Y Q Wang[1]

Beijing National Laboratory for Condensed Matter Physics, Institute of Physics, Chinese Academy of Sciences, PO Box 603, Beijing 100080, People's Republic of China

E-mail: yqwang@aphy.iphy.ac.cn

Received 8 February 2006
Published 24 March 2006
Online at stacks.iop.org/Nano/17/2073

Abstract
Silicon nanocrystals with well-controlled sizes below 5.0 nm at a number density up to 10^{12} cm^{-2} were directly grown in hydrogenated silicon oxide films by plasma-enhanced chemical vapour deposition using SiH_4, O_2 and H_2 as the precursor. For the immediate formation of silicon nanocrystals in deposits on a cold substrate, high-density hydrogen ions have to be maintained in the plasma. These innate silicon nanocrystals are found to be well isolated from each other and dispersed uniformly throughout the deposits. Intense visible photoluminescence was measured at room temperature from such samples, with the photon energy at about 1.67 eV being indifferent to the variation in particle size. The photoluminescence features can find a qualitative explanation in the nearly stabilized electronic states of silicon nanocrystals by Si=O surface-passivation.

1. Introduction

The fabrication of silicon-based light emitters is an urgent necessity for the development of integrated optoelectronics and photonics that is to employ procedures compatible with standard integration technology for microelectronics. Nanosized silicon particles embedded in appropriate compound matrices have proved to be one of the most promising candidates for this purpose [1–3]. In spite of the indirect band-gap for bulk crystal, silicon particles with diameters less than the Bohr radius of exciton (∼5 nm) have been made to exhibit intense visible photoluminescence (PL) owing to the quantum size effect. In recent years, the design structure that comprises of silicon nanocrystals in the robust SiO_2 matrix has attracted much attention [4–6] because of, among other beneficial factors, the excellent confinement effect of the oxide. Usually, the preparation of Si nanocrystals in the oxide matrix by chemical vapour deposition starts with a substoichiometric SiO_x ($x < 2$) layer, followed by subsequent thermal treatment. In so doing, the annealing temperature should be set at 1100 °C or even higher, so as to promote the precipitation and crystallization of silicon particles. In order to obtain an applicable light-emission (intense, of tunable wavelength and limited spectral width), clearly one expects a film with well isolated, uniformly dispersed silicon nanocrystals of variable size in narrow distribution. However, post-annealing at such a high temperature makes this rather unrealistic so that the irregular particle features from fast diffusion often result in an unwelcome broadening of the PL spectrum. On the other hand, it is shown that when the annealing temperature exceeds 950 °C, small crystallites coalesce into larger ones leading to a simultaneous reduction in the density of light-emitting particles [7]. This restricts both the wavelength and the quantum efficiency of the PL attainable. Nevertheless, such a high annealing temperature is unfavourable for optoelectronic integration since the unwanted diffusion of dopants thus induced would be unacceptable. It is essential to develop some alternative procedures using relatively low temperatures for the fabrication of light-emitting silicon nanostructures.

We have noticed that the local chemistry of the as-deposited silicon oxide films depends strongly on the preparation conditions. By changing the processing parameters, the deposit can be tuned between the two extremes either of well-separated Si and SiO_2 phases or of a homogeneous substoichiometric alloy $Si_{4-n}O_n$ ($n = 0$–4).

[1] Author to whom any correspondence should be addressed.

Theoretically, these are described by the random mixture model [8] and the random bonding model [9], respectively. If the silicon nanocrystals were grown immediately in the as-deposited film so that the features for both the particles and the compound matrix could be simultaneously determined once for all, this would save the notorious high-temperature post-annealing. It was reported that SiO_x films comprising of silicon nanocrystals could be synthesized by plasma-enhanced chemical vapour deposition (PECVD) at 300 °C [10] and 400 °C [11], however, the sizes of the crystals (6–10 nm [10] or 30–50 nm [11]) were quite large so no reports on measurable light emission were presented. In our earlier works, we reported that a very low substrate temperature was helpful for the formation of silicon nanoparticles, being exclusively amorphous there, of high number density in both the oxide and nitride compounds [12–14]. In the present paper, we demonstrate that high-density innate silicon nanocrystals can also be grown in the as-deposited oxide films, only a large proportion of hydrogen ions has to be maintained in the plasma for an effective concurrent chemical etching and/or hydrogen-mediated crystallization during deposition. For those deposits with silicon nanocrystals smaller than 5.0 nm, intense visible PL was measured at room temperature.

2. Experimental details

Silicon oxide films, about 0.5 μm thick, were deposited onto Si wafers and fused quartz substrates using capacitance-coupled PECVD with a SiH_4, O_2 and H_2 gas mixture. The flow ratio $r = [O_2]/([O_2] + [SiH_4])$ as the unique controlling parameter was varied from 0 to 0.5, while the summed flow rate for SiH_4 and O_2 was maintained at 2.0% of the total. At a working pressure of 1.0×10^2 Pa and a radiofrequency power density of 700 mW cm^{-2}, the resulting growth rate is estimated to be 5.0 nm min^{-1}. No intentional substrate heating was applied; the substrate temperature, altered solely by the plasma irradiation, was restricted below 60 °C by the end of the deposition. The local atomic environments and bonding configurations in the films were characterized by infrared absorption performed on a Perkin-Elmer 2000 Fourier-transform infrared (FTIR) system, and by inspecting the Si 2p line excited with Mg Kα radiation on an x-ray photoelectron spectrometer (ESCALab Mark-II). Formation of silicon nanocrystals in the films was verified by micro-Raman scattering, using a confocal laser Raman spectrometer (JY-6400). The size and spatial distribution of the embedded silicon nanocrystals were investigated on the bright-field images obtained with a Tecnai-20 transmission electron microscope (TEM). The PL at room temperature was excited using an Ar^+ laser operating at 514.5 nm, and was then detected using a CCD device within the wavelength range from 550 to 950 nm.

Under the given growth condition, silicon precipitates come about mainly due to the collision/clustering in the oxygen-ion deficient discharge, instead of being a solid-state process. The low-temperature of the substrate simply thwarts the subsequent diffusion process towards a homogenous substoichiometric deposit. Hence, by adjusting the precursor composition and/or the working pressure, the size of the silicon particles embedded in the compound matrix can be well controlled.

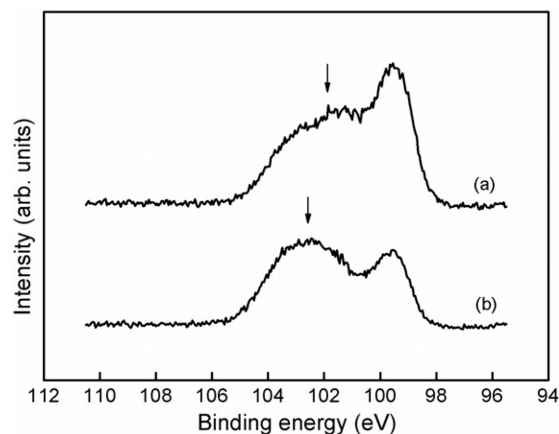

Figure 1. Si 2p line profile for the samples prepared with an oxygen fraction of (a) $r = 0.10$ and (b) $r = 0.20$. In both cases, an enunciated peak appears at ~99.5 eV, indicating the precipitation of silicon particles in the deposits.

3. Results and discussion

In the presence of abundant reductive hydrogen ions, the formation of silicon oxide films containing tiny silicon particles follows a complicated process of multiple reactions; therefore the chemical states of the final deposits are quite susceptible to the processing parameters. The hydrogen ions allow the occurrence of elemental silicon in deposits where, even with the oxygen fraction $r = 0.20$, the Si 2p line profile still exhibits a notable distinct peak at ~99.5 eV (figure 1), a photoelectron spectral fingerprint for elemental Si. This unambiguously suggests that phase separation is already under way in the as-deposited films. It is well known that in the silicon–oxygen bonds, charges transfer from the Si atoms to the electronegative O-atoms, resulting in a remarkable shift of binding energies for the Si core-levels. For materials comprising of Si^{n+}-ions of increasing ionicity (with 'n' up to 4), the corresponding binding energy for the Si 2p line changes continuously from 99.5 to 103.4 eV [15]. From figure 1, we see that as the oxygen fraction in the precursor is increased, the peak assigned to the oxidized states of Si atoms shifts towards a higher binding energy, and becomes dominant. It is heavily broadened with a full width at half maximum of about 2.0 eV, indicating the coexistence of varying ionic states for the oxidized Si atoms. This is also verifiable by the infrared transmittance measurement. In comparison with the pure hydrogenated silicon deposit, which exhibits only two features at around 640 and 2090 cm^{-1} characteristic of the wagging and stretching mode of $Si–H_2$ bonds, the FTIR spectrum for a typical silicon-rich oxide deposit, curve (b) in figure 2, generally manifests two more oxygen-related bands. The feature at about 450 cm^{-1} is assigned to the rocking mode of the Si–O bond, and the band extending from 700 to 1300 cm^{-1} can be decomposed into four components centred at about 780, 850, 980 and 1200 cm^{-1}, of which the peak at 850 cm^{-1} is identified as the bending mode of the $HSi–O_2Si$ and/or $HSi–O_3$ configurations, and the others are assigned to the bending and stretching modes of the Si–O bond. The feature at around 3350 cm^{-1} that is attributable to the O–H bond is weak. These observations confirm that the oxygen

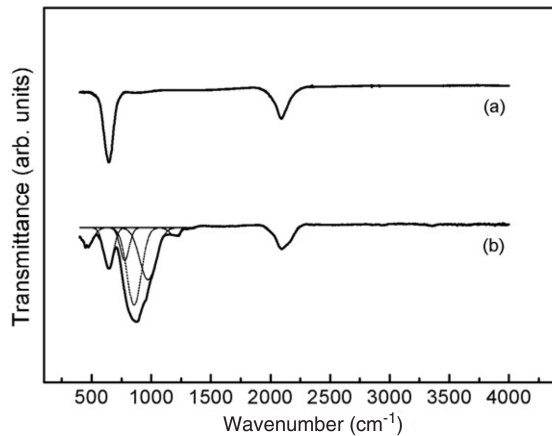

Figure 2. FTIR transmittance spectra for a pure hydrogenated silicon film (a) and for a Si-rich SiO_x deposit prepared with the oxygen fraction $r = 0.05$. Although much less oxygen was introduced in the precursor, the deposit is already characterized as Si-rich silicon oxide. The O–H bond at $\sim$3350 cm^{-1} is negligibly weak.

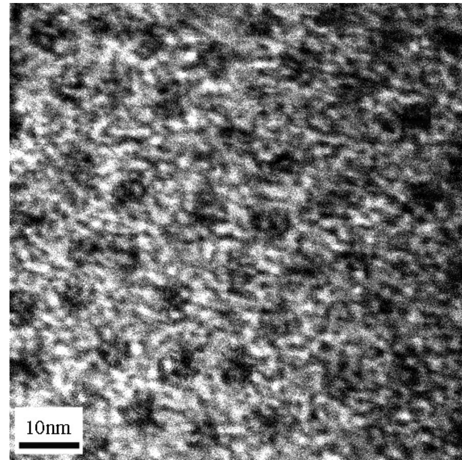

Figure 4. Plan-view TEM micrograph for a nc-Si-in-SiO_x sample prepared with the oxygen fraction $r = 0.10$. Distinct silicon particles (dark spots) of $\sim$5.0 nm in size are discernible. A number density of 1.06×10^{12} cm^{-2} was calculated.

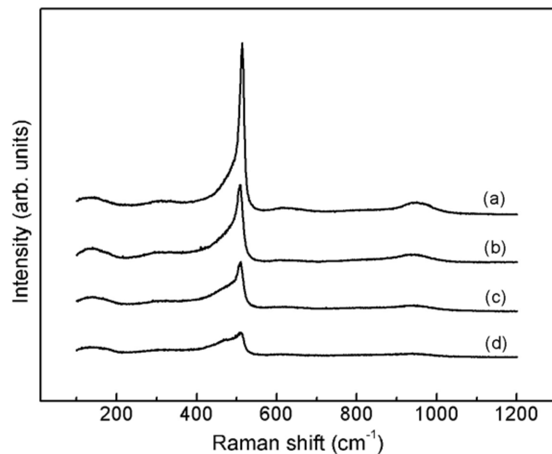

Figure 3. Micro-Raman spectra measured on the samples grown with different oxygen fractions in the precursor: (a) $r = 0.10$; (b) $r = 0.15$; (c) $r = 0.20$; (d) $r = 0.25$. The sharp peak at around 510 cm^{-1} is characteristic of silicon nanocrystals.

atoms can easily be incorporated into the films under the preparation conditions, and they exist mainly in the form of SiO_x units rather than bonding to the hydrogen atoms.

The nanocrystallinity of the tiny silicon particles in the as-deposited films is confirmed by the micro-Raman scattering measurement [16]. Figure 3 shows the Raman spectra of the samples prepared with different oxygen fractions r, of which the fluorescence background was fitted with a standard polynomial and subtracted. The sharp peak around 510 cm^{-1}, arising from the first-order Raman scattering of silicon phonons, confirms the presence of silicon particles in the as-grown oxide films in the form of nanocrystals. The significant red shift (i.e., softening of the phonon mode) and broadening of the Raman peak with respect to that for silicon bulk crystal are typical of the size effect in nanocrystals. It is clear to see that for more heavily oxidized samples, the line width of the Raman peak increases while its intensity quickly diminishes. This suggests a steady size reduction of the silicon nanocrystals, as can also be verified from the TEM micrographs. By taking into account the effect of both phonon confinement and elastic strain upon the Raman scattering of small crystals, the information of crystallite size can be extracted from the measured profiles [17]. The estimated average size of silicon nanocrystals in the samples is reduced from 4.4 to 2.3 nm with the value of r increasing from 0.10 to 0.25.

The existence of high number-density silicon nanocrystals in the as-deposited films is clearly confirmed by the bright-field TEM images. Figure 4 displays a typical plan-view TEM image of a sample prepared with $r = 0.10$. Well-separated silicon particles (dark spots) uniformly dispersed throughout the films, showing a narrow size distribution within 4.0–6.0 nm at a number density of about 1.06×10^{12} cm^{-2}. Note that the size of the silicon nanocrystals determined from the TEM images is somewhat larger than the data obtained on Raman scattering—a reasonable consequence due to the presence of amorphous clothing around the nanocrystals. This may explain the discrepancy in making the correlation between PL profiles and the size distribution of silicon particles, since the latter is often determined by different characterizing techniques.

Intense PL in the red region was observed at room temperature in all of the samples, wherein the averaged size of the silicon nanocrystals was smaller than 5.0 nm (figure 5). A remarkable enhancement of the PL intensity was achieved by increasing the oxygen fraction in the precursor, hence the oxygen concentration in the deposits. To our surprise, a difference by a factor of 20 was measured in the integral intensities for the curve (a) ($r = 0.10$) and curve (e) ($r = 0.25$), while the peak wavelength exhibits only a very moderate blue shift—it merely changes from 768 to 743 nm. Or, one can say that the PL is roughly pinned at the photon energy 1.61–1.67 eV. This is quite difficult to understand from a quantum confinement viewpoint, considering the nearly halved particle size and the only slightly increased particle density in these samples. Some other competitive recombination mechanisms such as those related to the interfacial states may operate in the photoluminescence from the current samples.

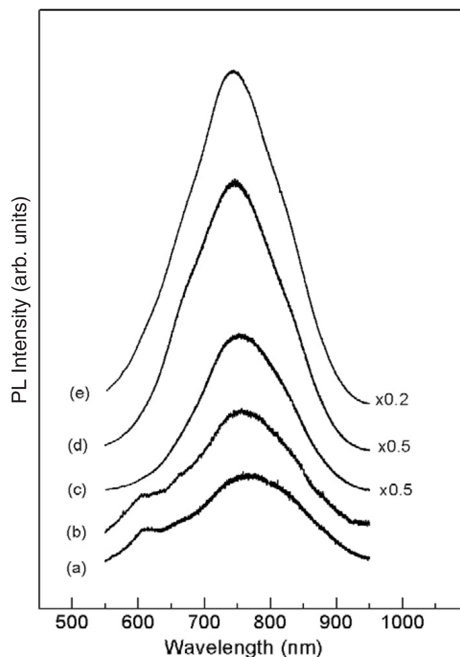

Figure 5. PL spectra from as-grown nc-Si-in-SiO_x samples prepared with varied oxygen fractions in the precursor: (a) $r = 0.10$; (b) $r = 0.12$; (c) $r = 0.15$; (d) $r = 0.20$; (e) $r = 0.25$.

In our previous publications, we reported the attainment of intensive PL across the whole visible light range in the Si-in-SiO_x and Si-in-SiN_x films prepared under similar processing conditions, where the silicon particles were entirely amorphous, and a clear correlation between the particle size and the peak wavelength of PL was recognizable qualitatively in accordance with the quantum confinement mechanism [12–14]. In the current samples, in which the silicon particles are nanocrystals, the PL photon energy seems stabilized, as in the case when the recombination proceeds via trapped exciton. Wolkin and coworkers [18] presented a detailed study on the possible PL mechanisms for crystalline silicon particles passivated with oxygen by calculating the electronic structures of such giant molecules [19]. They found that a stabilized electronic state, or even a trapped exciton may be formed on the Si=O double bonds, so that at particle sizes below 3.0 nm the PL photon energy increases very little. The photon energy (1.61–1.67 eV) versus the particle size measured here falls on the theoretical curve for the lowest transition in the presence of a Si=O double bond by Wolkin *et al*, but is smaller to the upper limit of the emission energy of 2.1 eV predicted by their calculation. Following Wolkin's model to treat the silicon particles in a compound matrix as giant molecules, of which the electronic structure is accordingly altered by the passivation at the boundary, the difference in the PL behaviour between the crystalline silicon nanoparticles and the amorphous ones seems understandable—in the latter case the electronic states might show an ever-increasing separation of the levels involved in optical transition with decreasing particle size. In the amorphous particles, optical transition other than from the trapped exciton states dominates due to the lack of long-range order within the particles.

From the FTIR spectra, we know that our samples contain quite a lot of hydrogen due to the low temperature growth condition, their PL profiles are, however, rather the same as the hydrogen-free samples prepared by high-temperature post-annealing [20]. This indicates that hydrogen-related bonds such as Si–O–H are less likely to be responsible for the observed PL, as was justified in the above discussions. For the samples with large silicon nanocrystals (figure 5, curves (a) and (b)), a minor peak at a fixed wavelength of about 605 nm becomes noticeable. This peak usually makes its presence in the PL from the SiO_2 layers implanted by Si [21, 22], which is attributed to a certain defect induced by ion damage in the oxide matrix. The significant enhancement in the PL efficiency for the silicon nanocrystal samples prepared with more oxygen in the precursor (figure 5, curves (d) and (e)) originates mainly in the substitution of Si–H passivation by Si=O double bonds.

Finally, we want to further discuss the growth of innate silicon nanocrystals in the oxide matrix at low substrate temperatures. The key factor for the immediate formation of silicon nanocrystals in the deposit is to maintain a high-density of hydrogen ions in the plasma; therefore the precursor has to be heavily diluted with hydrogen, and a large power-density has to be applied. The low substrate temperature facilitates the sustainment of phase separation, and, when there is insufficient hydrogen ions striking the growing surface, it results in a deposit of high-density amorphous silicon nanoparticles. With the preferential chemical etching to the strained Si–Si bonds and/or the crystallization mediated by hydrogen atoms, eventually the silicon particles that survive are crystalline. For a detailed discussion on the possible mechanisms, see [23] and references therein. This low temperature, high-density hydrogen ion procedure for the preparation of silicon nanocrystals in oxide, however, has one drawback: the ion-bombardment induced defects, perhaps also the hydrogen passivation at the boundary, are blamed for the relatively low PL efficiency—the highest external quantum efficiency for the samples here is estimated to be less than 1.0%. By further increasing the hydrogen ion proportion in plasma, we can achieve equally effective etching at a reduced ion energy, which can, at the same time, improve the optical quality of the deposits at a low growth rate. More elaborate work has to be done to establish an optimized growth procedure to obtain effective light-emitting silicon nanocrystals in an oxide matrix.

4. Summary

In summary, hydrogenated silicon-rich oxide films containing distinct innate silicon nanocrystals have been grown on cold substrates by a conventional plasma-enhanced chemical vapour deposition method using a hydrogen-diluted mixture of oxygen and silane as the precursor. The particle size can be reduced to below 5.0 nm, and the number density can be increased to 10^{12} cm^{-2}; consequently an intense light emission in the red region was measured at room temperature in this design structure. These results, while demonstrating a germane method for the preparation of composite nanostructures, largely reinforce the feasibility of fabricating silicon nanocrystal-based light-emitters in a procedure entirely compatible with modern very-large-scale integration technology.

Acknowledgment

The authors acknowledge financial support from the Natural Science Foundation of China (NSFC) under grant Nos 60306009, 50472070, 10404034 and 10574147.

References

[1] Seo S Y, Cho K S and Shin J H 2004 *Appl. Phys. Lett.* **84** 717
[2] Lacona F, Bongiorno C, Spinella C, Boninelli S and Priolo F 2004 *J. Appl. Phys.* **95** 3723
[3] Terranova M L, Piccirillo S, Sessa V, Botti S and Rossi M 1999 *Appl. Phys. Lett.* **74** 3146
[4] Wilkinson A R and Elliman R G 2004 *J. Appl. Phys.* **96** 4018
[5] Dal Negro L, Cazzanelli M, Danese B, Pavesi L, Iacona F, Franz G and Priolo F 2004 *J. Appl. Phys.* **96** 5747
[6] Fauchet P M, Ruan J, Chen H, Pavesi L, Dal Negro L, Cazzaneli M, Elliman R G, Smith N, Samoc M and Luther-Davies B 2005 *Opt. Mater.* **27** 745
[7] Kohli S, Theil J A, Dippo P C, Jones K M, Al-Jassim M M, Ahrenkiel R K, Rithner C D and Dorhout P K 2004 *Nanotechnology* **15** 1831–6
[8] Temkin R J 1975 *J. Non-Cryst. Solids* **17** 215
[9] Philipp H R 1972 *J. Non-Cryst. Solids* **8–10** 627
[10] Zhang X W 2005 *Phys. Status Solidi* a **202** 1773
[11] Lin C F, Tseng W T and Feng M S 2000 *J. Appl. Phys.* **87** 2808
[12] Wang Y Q, Chen W D, Liao X B and Cao Z X 2003 *Nanotechnology* **14** 1235
[13] Liu C, Li C R, Ji A L, Ma L B, Wang Y Q and Cao Z X 2005 *Appl. Phys. Lett.* **86** 223111
[14] Ma L B, Song R, Miao Y M, Li C R, Du Y, Wang Y Q and Cao Z X 2006 *Appl. Phys. Lett.* **88** 093102
[15] Himpsel F J, McFeely F R, Taleb-Ibrahimi A, Yarmoff J A and Hollinger G 1988 *Phys. Bev.* B **38** 6084
[16] Khiachtchev L, Räsänen M, Novikov S and Pavesi L 2004 *Appl. Phys. Lett.* **85** 1511
[17] Xia H, He Y L, Wang L C, Zhang W, Liu X N, Zhang X K and Feng D 1995 *J. Appl. Phys.* **78** 6705
[18] Wolkin M V, Jorne J, Fauchet P M, Allan G and Delerue C 1999 *Phys. Rev. Lett.* **82** 197
[19] Harwell D E, Croney J C, Qin W J, Thornton J T, Day J H, Hajime E K and Jameson D M 2003 *Chem. Lett.* **32** 1194
[20] Ma Z X, Liao X B, He J, Cheng W C, Yue G Z, Wang Y Q and Kong G L 1998 *J. Appl. Phys.* **83** 7934
[21] Song H, Bao X, Li N and Zhang L 1997 *J. Appl. Phys.* **82** 4028
[22] Im S, Jeong J Y, Oh M S, Kim H B, Chae K H, Whang C N and Song J H 1999 *Appl. Phys. Lett.* **74** 961
[23] Sriraman S, Agarwal S, Aydil E S and Maroudas D 2002 *Nature* **418** 62